An Adaptive Maximally Decimated Channelized UWB Receiver with Cyclic Prefix

Lei Feng, *Student member*, and Won Namgoong, *Member*

Abstract - **The frequency channelized receiver based on hybrid filter bank is a promising receiver structure for ultra-wideband (UWB) radio because of its relaxed circuit requirements and robustness to interference. The uncertainties in the analog analysis filters and the time varying nature of the propagation channels necessitate adaptive methods in practical frequency channelized receivers. Adaptive synthesis filters, however, suffer from slow convergence speed especially when maximally decimated to reduce the ADC sampling frequency. To improve the convergence speed, cyclic prefix (CP) is applied to the transmitted data. The propagation channel and the channelizer can then be modeled as a circulant matrix (CM) and block circulant matrix (BCM), respectively. Such matrix representation enables the transmitted data to be recovered by two cascaded one-tap equalizers, one of which corresponds to the channelizer and the other to the propagation channel. The cascaded structure is attractive as it allows the estimation of the propagation channel and the channelizer, which vary at vastly different rates, to be updated separately. Adaptive algorithms for both the fractionally spaced equalizer (FSE) and the symbol spaced equalizer (SSE) are derived. After initial convergence during startup, the adaptive performance of the channelized receiver to different propagation channels is similar to that of an ideal full band receiver.**

Index Terms - **Adaptive, channelized receiver, cyclic prefix, equalization, filter bank, ultra-wideband**

1 INTRODUCTION

UWB system is characterized by its huge signal bandwidth of generally several gigahertz. Since digitizing such a wideband signal at least at the signal Nyquist rate is difficult using a single ADC, parallel ADCs need to be employed. Maximally decimated frequency channelized receivers based on hybrid filter banks (HFB) achieve an effective sampling frequency that is M times the ADC sampling frequency, where M is the number of parallel ADCs [1]. Among the advantages of the frequency channelized receiver compared to the more conventional time channelized (i.e., time-interleaved ADC) receiver are the ease of designing the sample/hold circuitries, greater robustness to jitter/phase noise, and reduced ADC dynamic range requirements.

After passing through the analysis filters then sampling using parallel ADCs, an approach for detecting the received signal is to first reconstruct the channelized signal and then process the sampled full band signal as in the conventional receiver. Design of perfect reconstruction (PR) or approximately PR HFB has been explored [2][3]. A major challenge is that the digital synthesis filters require accurate knowledge of the transfer functions of the analog analysis filters, which may be unavailable in practice because of the uncertainties resulting from process and temperature variations.

The uncertainties in the analog analysis filters and the time varying nature of the propagation channels necessitate adaptive methods in practical frequency channelized receivers. Adaptive synthesis filters, however, suffer from slow convergence speed especially when maximally decimated [4][5]. As fast adaptive filter banks are required to quickly track variations in the wireless propagation channel, the slow convergence speed of the existing adaptive maximally decimated filter banks are ill-suited in UWB systems.

To achieve faster convergence, the proposed approach transmits blocks of data with cyclic prefix (CP). Cyclic prefixed data transmission is popular in both the multicarrier [6] and single carrier modulation [7] as it is efficient in combating intersymbol interference (ISI). Because of the large time dispersion caused by dense multipath propagation, transmission with CP is a promising approach in UWB systems. CP limits the matrix representation of the propagation channel to a circulant matrix (CM) subspace instead of the space for all possible channel models. The CM subspace matrices can be decomposed into the multiplication of two fixed DFT/IDFT matrices and a diagonal matrix, which can be compensated by a set of one-tap equalizers. Two primary examples of communication systems that exploit the structural properties of the CM are cyclic prefixed single carrier (CP-SC) and orthogonal frequency division multiplexing (OFDM) systems. Their main difference is that OFDM, unlike in CP-SC, employs an IDFT operation at the transmitter, resulting in large transmit power peak-to-average ratio (PAR) [8]. Although the reception technique proposed in this paper is equally applicable to both CP-SC and OFDM systems, we focus on CP-SC system because of the smaller PAR. A smaller PAR generally indicates more efficient power usage and simplified power amplifier design, which is a major implementation challenge in UWB radio [9].

In this paper, we show that as in the full band receiver, CP data transmission also simplifies the detection process of

Manuscript received June 2004; Revised December 2004.

This work was supported in part by the Army Research Office under contract number DAAD19-01-1-0477 and National Science Foundation under contract number ECS-0134629.

The authors are with the department of Electrical Engineering, University of Southern California, Los Angeles, CA 90007 USA (email: leifeng@usc.edu, namgoong@usc.edu)

the frequency channelized receiver. The frequency channelizer can be modeled as a block circulant matrix (BCM), which is a generalization of a CM. A BCM becomes a CM if the number of channels in the channelizer is one, which corresponds to the conventional full band receiver. The properties of BCM were investigated in [10] and [11] for applications in electromagnetics. In the BCM subspace, all matrices can be decomposed into two fixed DFT related matrices and a block diagonal matrix [10]. Additional simplification is possible by exploiting the structure of subband filters to further decompose the channelized receiver into three fixed DFT related matrices and a diagonal matrix. Since the propagation channel is modeled as a CM, the channelized receiver detection can be achieved by two cascaded sets of one-tap equalizers and several DFT/IDFT related operations. The use of one-tap equalizers simplifies the estimation process, resulting in faster convergence speed.

Adaptive algorithms for the frequency channelized receiver based on fractionally spaced equalizer (FSE) and symbol spaced equalizer (SSE) are derived. Compared to when SSE is employed, receivers using FSE achieve improved steady-state performance but suffer from slower convergence speed. In both the FSE and SSE based channelized receivers, the receiver adaptively compensates the propagation channel and the channelizer separately, each of which vary at vastly different rates. The one-tap equalizers for the frequency channelizer can be fixed or updated very slowly to track variations in the analog analysis filters after initial convergence. The adaptive receiver then operates as if its input is from an ideal full band receiver, resulting in fast tracking of propagation channel variations. All constant matrices in the adaptive algorithms can be efficiently realized using FFT/IFFT as they are all related to the DFT/IDFT operation. Simulation shows the channelized receiver using FSE (or SSE) achieves about the same performance as that of a conventional ideal full band receiver using FSE (or SSE).

The paper is organized as follow. Section II describes the system model. The general cascaded one-tap equalizer structure is introduced in Section III. Section IV derives the cascaded adaptive algorithms for both the FSE and SSE channelized receivers. Section V provides simulation results and conclusions are drawn in Section VI.

2 SYSTEM MODEL

Assuming a block of K_b consecutive symbols are transmitted, the received UWB signal $r_{rec}(t)$, which is real, is

$$r_{rec}(t) = \sum_{k=0}^{K_b-1} a_k p(t-kT) + v(t) \qquad (1)$$

where a_k is the kth transmitted antipodal data, T is the symbol period, $p(t)$ is the real propagation channel response, and $v(t)$ is the additive white Gaussian noise (AWGN). In CP-SC system, a certain number of symbols at the end of each block are copied and appended to the beginning of the block to form CP. The length of the CP is set to exceed the impulse response of the propagation channel. Assuming K data symbols are transmitted in each block, there are $(K_b - K)$ CP symbols.

The UWB system with the frequency channelized receiver is shown in Fig. 1. The channelized receiver consists of two parts: analog channelizer and digital equalizer. When viewed as a HFB, the channelizer is the continuous-time analysis filter and the digital equalizer is the discrete synthesis filter. The purpose of the channelizer is to decompose the received signal into multiple frequency subbands so that the ADC requirements are relaxed. The digital equalizer then compensates for the distortion caused by the channelizer and the propagation channel to detect the transmitted data.

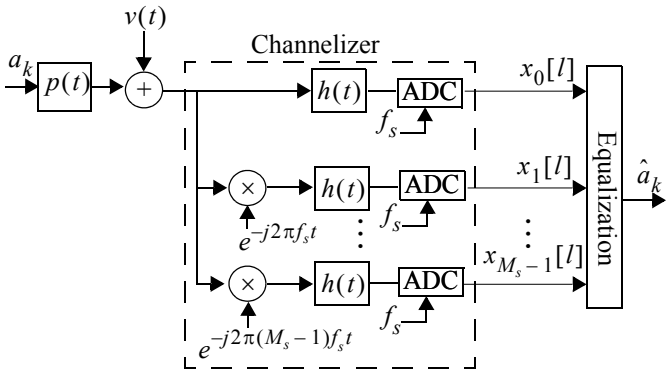

Fig. 1 The UWB system with frequency channelized receiver.

As shown in Fig. 1, the received signal $r_{rec}(t)$ is downconverted by a set of M_s equally spaced mixers $e^{-j2\pi m f_s t}$ ($m = 0, \ldots, M_s - 1$, $f_s = 1/T_s$). The downconverted signals are passed through a bank of M_s continuous-time lowpass analysis filters $\{h(t)\}$, then sampled by ADCs at a rate of $1/T_s$ to produce the digitized data $x_m[l]$. Since there are $M = 2M_s - 1$ ADCs (one ADC in the zeroth subband and two ADCs in each nonzero subbands), the effective sampling frequency of the receiver is $1/T_e = M/T_s$. To obtain sufficient statistics, the effective sampling frequency must be greater than the Nyquist rate of the received UWB signal. Assuming the signal is bandlimited to $2/T$, the effective sampling frequency is set to be $1/T_e = 2/T$ in this paper. The digital equalizer then operates on $x_m[l]$ to produce the estimated output data $\hat{a}_k$.

To obtain the discrete equivalent model of the system in Fig. 1, which is subsequently used for simulation and analysis, the received signal $r_{rec}(t)$ is sampled at κ/T_e, where κ is a positive integer. Since $\{h(t)\}$ and $r_{rec}(t)$ are bandlimited, the discrete model is accurate for sufficiently large κ. The discrete equivalent model is obtained by oversampling $r_{rec}(t)$, because the continuous-time convolution in the channelizer can then be modeled as a discrete-time convolution. Such discrete-time modeling enables us to exploit the structure of the corresponding matrix representation to produce an efficient one-tap digital equalizer as will become clear in later sections. Although $\kappa = 4$ is used when simulating for accuracy in our discrete equivalent model, we assume $\kappa = 1$ for simplicity when analyzing the frequency channelized receiver. This is a reasonable assumption since $r_{rec}(t)$ and the channelizer are approximately bandlimited within $1/(2T_e)$. Applying the equivalence theorem of the dig-

ital and analog signal processing [13], the lth sample of the mth subband is

$$x_m[l] = \{e^{j\varphi_m}e^{-j2\pi mf_s t}r_{rec}(t)\} \otimes h(t)|_{t=lT_s} = e^{j\varphi_m}\sum_{k=0}^{K_b-1} a_k\left(\sum_{n'} p[lM-n'-2k]h_m[n']\right) + v_m[l] \quad (2)$$

where φ_m is the initial phase of the mth mixer, $\otimes$ denotes the convolution operation, $p[n'] = p(n'T_e)$, $h_m[n'] = T_e h(n'T_e)e^{j2\pi mn'/M}$ and $v_m[l] = \{e^{j\varphi_m}e^{-j2\pi mf_s t}v(t)\} \otimes h(t)|_{t=lT_s}$. When maximally decimated, the effect of the mixer and lowpass filter can be readily shown to be equivalent to filtering by $h_m[n']$. We assume for simplicity that the mixers are designed so that $\varphi_0 = \varphi_1 = \ldots = \varphi_{M_s-1} = 0$ in the remaining part of the paper. The proposed reception approach can be readily modified to account for the more general case with arbitrary initial phase values. The subband noise $v_m[l]$ is modeled as a discrete white noise $v[n]$ passing through $h_m[n']$, where $v[n]$ is the AWGN with a PSD that corresponds to that of $v(t)$.

In (2), the expression for $x_m[l]$ can be simplified by first defining $s[n]$ as

$$s[n] = \begin{cases} a_{n/2} & , n \text{ is even} \\ 0 & , n \text{ is odd} \end{cases} \quad (3)$$

$x_m[l]$ can then be written as

$$x_m[l] = \sum_{n'} r[lM-n']h_m[n'] + v_m[l] \quad (4)$$

where

$$r[n] = \sum_{n'=0}^{2K_b-1} p[n-n']s[n'] \quad (5)$$

Using (4), the discrete equivalent model for the mth subband is shown in Fig. 2, where the different sampling rates for each section are indicated at the bottom.

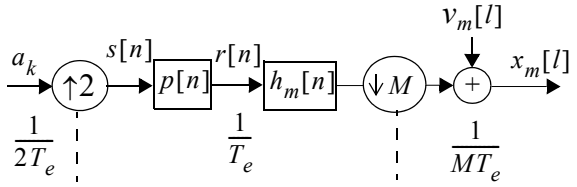

Fig. 2 A discrete equivalent model of the mth subband.

Although $x_m[l]$ $(m = 0, \ldots, M_s-1)$ provide sufficient statistics of the UWB signal, the discrete spectrum covered by the M_s subbands is mainly between 0 and π. To form a complete representation of the received signal, $M = 2M_s-1$ subbands between 0 and 2π are needed. Since the received signal is assumed to be real, the remaining spectrum is obtained by conjugating the M_s-1 nonzero subbands. These subbands are virtual subbands as they are not actually implemented but are used to simplify the analysis. For subbands $m = M_s, \ldots, 2M_s-2$, the conjugated samples and the corresponding analysis filters are

$$x_m[l] = x_{M-1-m}{}^*[l] \quad (6)$$

$$h_m[n'] = h_0[n']e^{j2\pi mn/M} \quad (7)$$

We will subsequently use $M = 2M_s-1$ subbands instead of M_s subbands for analysis.

3 GENERAL EQUALIZER STRUCTURE

In this section, the general cascaded equalizer structure for the channelized receiver is developed. Towards this end, we first represent the propagation channel and the channelizer as a CM and BCM, respectively. Such matrix representations are possible because of the CP in the transmission blocks. Both matrices are then diagonalized, so that one-tap equalizers can be employed. Based on the diagonal decomposition, the cascaded equalizer structure is derived.

3.1 Matrix representation of channel and channelizer

When CP transmission is employed, it is well known that the propagation channel can be modeled as a circulant matrix. Assuming $2K = MN$, where N is the number of samples collected in each subband and K is the number of data symbols in a transmission block, the CM of the propagation channel is

$$\mathbf{P} = \begin{bmatrix} p[0] & p[MN-1] & \ldots & p[1] \\ \ldots & \ldots & \ldots & \ldots \\ p[MN-2] & \ldots & p[0] & p[MN-1] \\ p[MN-1] & \ldots & p[1] & p[0] \end{bmatrix} \quad (8)$$

Denoting the upsampled data symbols in a transmission block as $\mathbf{s} = [s[0], s[1], \ldots, s[NM-1]]^T$, where T denotes transpose, the received signal vector is

$$\mathbf{r} = [r[0], \ldots, r[NM-1]]^T = \mathbf{Ps} \quad (9)$$

After passing through the channelizer, the nth sample of all M subbands $(n = 0, \ldots, N-1)$ in vector form is $\mathbf{x}[n] = [x_0[n], x_1[n], \ldots, x_{M-1}[n]]^T$ and the corresponding noise is $\mathbf{v}_s[n] = [v_0[n], v_1[n], \ldots, v_{M-1}[n]]^T$. The $(N-1)$th sample of all M subbands can be expressed as

$$\mathbf{x}[N-1] = \begin{bmatrix} h_0[MN-1] & \ldots & h_0[1] & h_0[0] \\ h_1[MN-1] & \ldots & h_1[1] & h_1[0] \\ \ldots & \ldots & \ldots & \ldots \\ h_{M-1}[MN-1] & \ldots & h_{M-1}[1] & h_{M-1}[0] \end{bmatrix} \mathbf{r} + \mathbf{v}_s[N-1] = \begin{bmatrix} \mathbf{H}_{N-1} & \ldots & \mathbf{H}_1 & \mathbf{H}_0 \end{bmatrix} \mathbf{r} + \mathbf{v}_s[N-1] \quad (10)$$

where $\mathbf{H}_n$ are $M \times M$ matrices. All the subband samples in a transmission block, denoted as $\mathbf{x} = [\mathbf{x}[0]^T, \ldots, \mathbf{x}[N-1]^T]^T$, is represented as

$$\mathbf{x} = \mathbf{Hr} + \mathbf{v}_s = \mathbf{HPs} + \mathbf{v}_s \quad (11)$$

where $\mathbf{v}_s = [\mathbf{v}_s[0]^T, \mathbf{v}_s[1]^T, \ldots, \mathbf{v}_s[N-1]^T]^T$ is the noise vector, and $\mathbf{H}$ is a block circulant matrix defined as

$$\mathbf{H} = \begin{bmatrix} \mathbf{H}_0 & \mathbf{H}_{N-1} & \cdots & \mathbf{H}_1 \\ \mathbf{H}_1 & \mathbf{H}_0 & \cdots & \mathbf{H}_2 \\ \cdots & \cdots & \cdots & \cdots \\ \mathbf{H}_{N-2} & \cdots & \mathbf{H}_0 & \mathbf{H}_{N-1} \\ \mathbf{H}_{N-1} & \cdots & \mathbf{H}_1 & \mathbf{H}_0 \end{bmatrix} \tag{12}$$

3.2 Diagonalizing channel and channelizer matrices

To achieve fast and efficient detection using one-tap equalizers, both the channel matrix **P** in (8) and the channelizer matrix **H** in (12) need to be decomposed as diagonal matrices. As **P** is a circulant matrix (CM), diagonalizing it is straightforward. **P** can be decomposed as

$$\mathbf{P} = \mathbf{F}^{-1}\Lambda\mathbf{F} \tag{13}$$

In (13), Λ is a diagonal matrix, and $\mathbf{F} = [W_{MN}^{-kn}]$ $(k, n = 0, \ldots, MN-1)$ is the DFT matrix, where $W_{MN}^{-kn} = e^{-j2\pi kn/(MN)}$.

Unlike **P**, **H** is a block circulant matrix (BCM). Applying the results of BCM decomposition in [10], **H** can be decomposed as

$$\mathbf{H} = \mathbf{F}_B^{-1}\mathbf{D}\mathbf{F}_B \tag{14}$$

In (14), the DFT related matrices $\mathbf{F}_B = [W_N^{-kn}\mathbf{I}_M]$, $\mathbf{F}_B^{-1} = [W_N^{kn}\mathbf{I}_M]/N$, $(k, n = 0, \ldots, N-1)$, where $\mathbf{I}_M$ is a $M \times M$ identity matrix. **D** is a block diagonal matrix $\mathbf{D} = \mathbf{diag}(\mathbf{H}^{(0)}, \ldots, \mathbf{H}^{(N-1)})$, where **diag**( ) denotes a block diagonal matrix with the matrices inside the parenthesis on the diagonal. $\mathbf{H}^{(k)}$ is related to $\mathbf{H}_n$ in (12) by DFT/IDFT operations

$$\mathbf{H}^{(k)} = \sum_{n=0}^{N-1} \mathbf{H}_n W_N^{-kn}, \quad \mathbf{H}_n = \frac{1}{N}\sum_{k=0}^{N-1} \mathbf{H}^{(k)} W_N^{kn} \tag{15}$$

To diagonalize **D**, which is a block diagonal matrix, we exploit the structure of the channelizer. As shown in (7), the subband responses in a channelizer are modulated versions of a template lowpass filter response. Then, block $\mathbf{H}_n$ in **H** can be decomposed as

$$\mathbf{H}_n = \begin{bmatrix} h_0[(n+1)M-1] & \ldots & h_0[nM] \\ W_M^{M-1} h_0[(n+1)M-1] & \ldots & h_0[nM] \\ \cdots & \cdots & \cdots \\ W_M^{(M-1)^2} h_0[(n+1)M-1] & \ldots & h_0[nM] \end{bmatrix}$$

$$= \mathbf{F}_M \mathbf{H}_n^d \tag{16}$$

where

$$\mathbf{F}_M = \begin{bmatrix} 1 & \ldots & 1 & 1 \\ W_M^{M-1} & \ldots & W_M^1 & 1 \\ \cdots & \cdots & \cdots & \cdots \\ W_M^{(M-1)^2} & \ldots & W_M^{M-1} & 1 \end{bmatrix} \tag{17}$$

$$\mathbf{H}_n^d = diag(h[(n+1)M-1], \ldots, h[nM]) \tag{18}$$

diag( ) denotes a diagonal matrix with elements in the parenthesis on the diagonal. Using (16), $\mathbf{H}^{(k)}$ in (15) can then be written as

$$\mathbf{H}^{(k)} = \sum_{n=0}^{N-1} \mathbf{H}_n W_N^{-kn} = \mathbf{F}_M \sum_{n=0}^{N-1} \mathbf{H}_n^d W_N^{-kn} \tag{19}$$

From (19), $\mathbf{D} = \mathbf{diag}(\mathbf{H}^{(0)}, \ldots, \mathbf{H}^{(N-1)})$ can be decomposed as

$$\mathbf{D} = \mathbf{F}_D\mathbf{C} \tag{20}$$

where

$$\mathbf{F}_D = \mathbf{diag}(\mathbf{F}_M, \ldots, \mathbf{F}_M) \tag{21}$$

$$\mathbf{C} = \mathbf{diag}\left(\sum_{n=0}^{N-1} \mathbf{H}_n^d, \sum_{n=0}^{N-1} \mathbf{H}_n^d W_N^{-n}, \ldots, \sum_{n=0}^{N-1} \mathbf{H}_n^d W_N^{-n(N-1)}\right) \tag{22}$$

C is a diagonal matrix because $\mathbf{H}_n^d$ are all diagonal matrices. The BCM channelizer matrix **H** then becomes

$$\mathbf{H} = \mathbf{F}_B^{-1}\mathbf{F}_D\mathbf{C}\mathbf{F}_B \tag{23}$$

where **C** is a diagonal matrix and $\mathbf{F}_B$, $\mathbf{F}_B^{-1}$, and $\mathbf{F}_D$ are DFT/IDFT related matrices.

3.3 Cascaded equalizer structure

From (11), **s** can be estimated by multiplying **x** with $\mathbf{P}^{-1}\mathbf{H}^{-1}$. Inverting (13) and (23), $\mathbf{P}^{-1}\mathbf{H}^{-1} = \mathbf{F}^{-1}\Lambda^{-1}\mathbf{F}\mathbf{F}_B^{-1}\mathbf{C}^{-1}\mathbf{F}_D^{-1}\mathbf{F}_B$. To avoid noise enhancement, diagonal matrices $\mathbf{C}^{-1}$ and Λ^{-1} are replaced by equalizers $\mathbf{C}_e^H$ and Λ_e^H, respectively, where the superscript *H* stands for conjugate transpose. Both $\mathbf{C}_e^H$ and Λ_e^H are diagonal matrices. The estimate of **s** then becomes

$$\hat{\mathbf{s}} = \mathbf{F}^{-1}\Lambda_e^H\mathbf{F}\mathbf{F}_B^{-1}\mathbf{C}_e^H\mathbf{F}_D^{-1}\mathbf{F}_B\mathbf{x} \tag{24}$$

In (24), all matrices are DFT/IDFT related matrices, except for $\mathbf{C}_e$ and Λ_e, which are both diagonal matrices. The elements in $\mathbf{C}_e$ and Λ_e can be determined adaptively as described in the following section. $\mathbf{C}_e$ and Λ_e represent one-tap equalizers for the channelizer and the propagation channel, respectively. This decomposition reduces the number of parameters to estimate, resulting in faster convergence speed. More importantly, the estimation of the propagation channel and the channelizer, which vary at vastly different rates, can be updated separately. As a result, the adaptive performance of a maximally decimated channelized receiver can be made similar to an ideal full band receiver after initial convergence during startup.

4 ADAPTIVE CASCADED EQUALIZERS

As the effective sampling frequency is chosen to be twice the symbol rate, both equalizers in (24) are FSEs. To achieve faster convergence at the cost of performance loss [14], the propagation channel equalizer can be modified to be a SSE. In this section, adaptive algorithms for both the FSE and SSE are derived. Adapting the equalizer structure in (24) is not straightforward because the equalizers are cascaded. The adaptive algorithm are derived to minimize the minimum mean squared error.

4.1 Fractional Spaced Equalizer

Since only half of the elements in $\hat{\mathbf{s}}$ correspond to the transmitted data, the data $\mathbf{a} = [a_0, a_1, \ldots, a_{K-1}]^T$ can be recovered by dropping every other row of $\mathbf{F}^{-1}$. Defining $\mathbf{F}_{1/2}^{-1} = [W_{MN/2}^{kn}]/(MN/2)$, $(k, n = 0, \ldots, MN/2 - 1)$ and

$$\Lambda_e = \begin{bmatrix} \Lambda_{e0} & \mathbf{0} \\ \mathbf{0} & \Lambda_{e1} \end{bmatrix} \tag{25}$$

where Λ_{e0} and Λ_{e1} are $\left(\frac{MN}{2} \times \frac{MN}{2}\right)$ diagonal matrices, the estimate of $\mathbf{a}$ is obtained as

$$\begin{aligned} \hat{\mathbf{a}} &= \frac{1}{2}\begin{bmatrix} \mathbf{F}_{1/2}^{-1} & \mathbf{F}_{1/2}^{-1} \end{bmatrix} \begin{bmatrix} \Lambda_{e0}^H & \mathbf{0} \\ \mathbf{0} & \Lambda_{e1}^H \end{bmatrix} \mathbf{F}\mathbf{F}_B^{-1}\mathbf{C}_e^H\mathbf{F}_D^{-1}\mathbf{F}_B\mathbf{x} \\ &= \frac{1}{2}\mathbf{F}_{1/2}^{-1}\begin{bmatrix} \Lambda_{e0}^H & \Lambda_{e1}^H \end{bmatrix} \mathbf{F}\mathbf{F}_B^{-1}\mathbf{C}_e^H\mathbf{F}_D^{-1}\mathbf{F}_B\mathbf{x} \end{aligned} \tag{26}$$

Each output of $\begin{bmatrix} \Lambda_{e0}^H & \Lambda_{e1}^H \end{bmatrix}$ is a summation of two one-tap equalizer outputs, since FSE is employed [12] and the effective sampling frequency is twice the symbol frequency.

An adaptive algorithm for the equalizer in (26) is derived to minimize the mean squared error (MSE). Defining the detection error as

$$\mathbf{e}_a = \mathbf{a} - \hat{\mathbf{a}} \tag{27}$$

The MSE of a block of signals is the expectation of $\mathbf{e}_a^H\mathbf{e}_a$. Since expectations are typically obtained by instantaneous estimations in adaptive algorithms such as in the LMS algorithm, the derivation is directly based on the squared error

$$J = \mathbf{e}_a^H\mathbf{e}_a \tag{28}$$

According to the method of steepest descent, the two equalizers can be updated with the corresponding gradients. Denote the diagonal elements of the equalizer Λ_e and $\mathbf{C}_e$ as column vectors λ and $\mathbf{c}$, respectively. The gradient vectors are defined as

$$\nabla_\lambda J = 2\frac{\partial J}{\partial \lambda^*} \quad \nabla_c J = 2\frac{\partial J}{\partial \mathbf{c}^*} \tag{29}$$

The procedure for deriving the gradients of FSE is provided in the APPENDIX. The results are

$$\nabla_\lambda J = -\left(\mathbf{u}_\lambda \bullet \begin{bmatrix} \mathbf{e}_\lambda \\ \mathbf{e}_\lambda \end{bmatrix}^*\right) \tag{30}$$

$$\nabla_c J = -\mathbf{u}_c \bullet \mathbf{e}_c^* \tag{31}$$

where $\bullet$ denotes the inner product operation, i.e., element-wise multiplication. In (30), the input to the equalizer Λ_e is

$$\mathbf{u}_\lambda = \mathbf{F}\mathbf{F}_B^{-1}\mathbf{C}_e^H\mathbf{F}_D^{-1}\mathbf{F}_B\mathbf{x} \tag{32}$$

and the corresponding output error is

$$\mathbf{e}_\lambda = (\mathbf{F}_{1/2}^{-1})^H\mathbf{a} - \frac{1}{MN}\begin{bmatrix} \Lambda_{e0}^H & \Lambda_{e1}^H \end{bmatrix}\mathbf{F}\mathbf{F}_B^{-1}\mathbf{C}_e^H\mathbf{F}_D^{-1}\mathbf{F}_B\mathbf{x} \tag{33}$$

Similarly in (31), the input to the equalizer $\mathbf{C}_e$ is

$$\mathbf{u}_c = \mathbf{F}_D^{-1}\mathbf{F}_B\mathbf{x} \tag{34}$$

and the corresponding output error is

$$\mathbf{e}_c = (\mathbf{F}_B^{-1})^H\mathbf{F}^H\begin{bmatrix} \Lambda_{e0}^H & \Lambda_{e1}^H \end{bmatrix}^H\mathbf{e}_\lambda \tag{35}$$

The gradients can be applied to the adaptive algorithms by introducing data block index τ as the iteration index. By appending τ to all the signals (e.g. $\mathbf{x}(\tau)$, $\mathbf{C}_e^H(\tau)$, $\mathbf{u}_\lambda(\tau)$, $\mathbf{e}_\lambda(\tau)$, etc.), the adaptive equations are

$$\begin{aligned} \mathbf{c}(\tau+1) &= \mathbf{c}(\tau) + \mu_c[-\nabla_c J] \\ &= \mathbf{c}(\tau) + \mu_c\mathbf{u}_c(\tau) \bullet \mathbf{e}_c(\tau)^* \end{aligned} \tag{36}$$

$$\begin{aligned} \lambda(\tau+1) &= \lambda(\tau) + \mu_\lambda[-\nabla_\lambda J] \\ &= \lambda(\tau) + \mu_\lambda\mathbf{u}_\lambda(\tau) \bullet \begin{bmatrix} \mathbf{e}_\lambda(\tau) \\ \mathbf{e}_\lambda(\tau) \end{bmatrix}^* \end{aligned} \tag{37}$$

where μ_c and μ_λ are the update step sizes for the channelizer and propagation channel equalizers, respectively. The FSE adaptive structure is shown in Fig. 3.

The cascaded equalizer structure enables the receiver to track the variations in the propagation channel and the channelizer at different rates. This decomposition is important as the channelizer and the propagation channel vary at vastly different rates. After the initial convergence of $\mathbf{C}_e$, which is achieved after turning on the receiver, the receiver basically adapts only equalizer Λ_e, resulting in performance comparable to an ideal receiver for CP-SC system.

4.2 Symbol Spaced Equalizer

The convergence speed can be further improved by employing a SSE for the propagation channel. A filter matched to the transmitted pulse filters the output of the channelizer equalizer. The output of the matched filter is then decimated to the symbol rate before passing through the propagation channel SSE. The use of SSE introduces additional performance loss because the matched filter before decimation is matched to

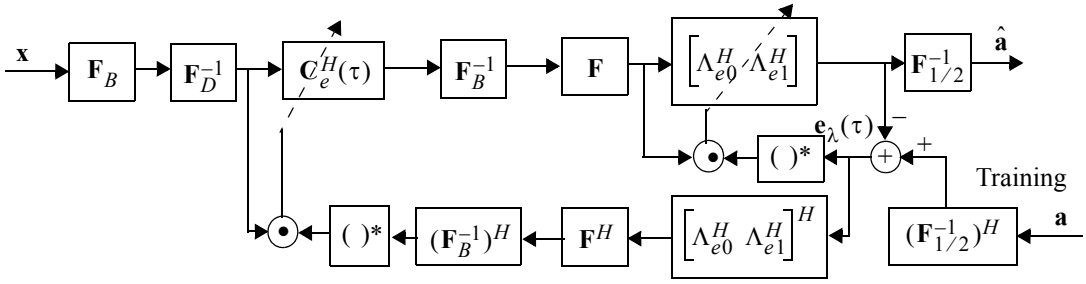

Fig. 3 Cascaded adaptive equalizers.

the transmit pulse and not to the channel pulse response, which is unknown at the receiver. As a result, the decimated samples do not provide sufficient statistics for the propagation channel equalizer, resulting in performance loss.

The matched filter is represented as a $MN/2 \times MN$ matrix, which is obtained by dropping every other row of a CM constructed with the transmitted pulse response. As in (26), the matched filter matrix can be decomposed as $\mathbf{F}_{1/2}^{-1}\left[\rho_0^H \ \rho_1^H\right]\mathbf{F}/2$, where ρ_0 and ρ_1 are constant diagonal matrices corresponding to the matched filter. As the dimensions of the matched filter matrix is $MN/2 \times MN$, the subsequent propagation channel equalizer is a SSE and is given by $\mathbf{F}_{1/2}^{-1}\Lambda_s^H\mathbf{F}_{1/2}$. The transmitted data are estimated as

$$\hat{\mathbf{a}} = \frac{1}{2}\mathbf{F}_{1/2}^{-1}\Lambda_s^H\left[\rho_0^H \ \rho_1^H\right]\mathbf{F}\mathbf{F}_B^{-1}\mathbf{C}_e^H\mathbf{F}_D^{-1}\mathbf{F}_B\mathbf{x} \tag{38}$$

The gradients of the cost function J on the equalizer taps of Λ_s and $\mathbf{C}_e$ are $\nabla_{s\lambda}J$ and $\nabla_{sc}J$, respectively. Derivation of the SSE gradients is provided in the APPENDIX.

The adaptive equations for SSE is similar to those for FSE. The input and the error signal of the two equalizers are

$$\mathbf{u}_{s\lambda} = \left[\rho_0^H \ \rho_1^H\right]\mathbf{F}\mathbf{F}_B^{-1}\mathbf{C}_e^H\mathbf{F}_D^{-1}\mathbf{F}_B\mathbf{x} \tag{39}$$

$$\mathbf{e}_{s\lambda} = (\mathbf{F}_{1/2}^{-1})^H\mathbf{a} - \frac{1}{MN}\Lambda_s^H\left[\rho_0^H \ \rho_1^H\right]\mathbf{F}\mathbf{F}_B^{-1}\mathbf{C}_e^H\mathbf{F}_D^{-1}\mathbf{F}_B\mathbf{x} \tag{40}$$

$$\mathbf{u}_{sc} = \mathbf{F}_D^{-1}\mathbf{F}_B\mathbf{x} \tag{41}$$

$$\mathbf{e}_{sc} = (\mathbf{F}_B^{-1})^H\mathbf{F}^H\left[\rho_0^H \ \rho_1^H\right]^H\Lambda_s\mathbf{e}_\lambda \tag{42}$$

Defining $\mathbf{c}(\tau)$ and $\lambda(\tau)$ as the vector form of equalizer taps of $\mathbf{C}_e$ and Λ_s, respectively, the adaptive equations are

$$\mathbf{c}(\tau+1) = \mathbf{c}(\tau) + \mu_c\mathbf{u}_{sc}(\tau) \bullet \mathbf{e}_{sc}(\tau)^* \tag{43}$$

$$\lambda(\tau+1) = \lambda(\tau) + \mu_\lambda\mathbf{u}_{s\lambda}(\tau) \bullet \mathbf{e}_{s\lambda}(\tau)^* \tag{44}$$

5 SIMULATION RESULTS

The transmitted data is modulated by a raised cosine pulse with a roll off factor of 0.8. The symbol period is 0.5ns. The effective sampling rate is two samples per symbol (i.e., 4GS/s). The UWB channel model is CM1 model proposed by IEEE P802.15 working group.

The channelized receiver is composed of $M_s = 4$ subbands so that the effective sampling frequency is seven times the subband ADC sampling frequency. The analog prototype filter is a fourth order Butterworth lowpass filter whose cutoff frequency is half of the ADC sampling frequency. Since most of the multipath energy is within the first 20ns, the CP period is selected to be 20ns. Each data block includes 280 information bits and 42 CP bits. In addition to the channelized receiver, the performance of an ideal full band CP-SC receiver that samples the received signal at twice the symbol frequency of 4GS/s is included for comparison. The signal energy is $E_b = \sum_n (p[n])^2$, and the noise power $N_0/2$ is the variance of $v[n]$. As SSE is sensitive to the sampling time [14], the sampling time of SSE is selected to achieve the best performance.

LMS algorithm is applied to the channelized and full band receiver structures. The convergence speeds of the FSE and SSE are compared for the channelized and full band receivers. The channelized receiver performance is considered for two different modes of operation -- startup and transition modes. In the startup mode, the receiver has no prior knowledge of the propagation channel or the channelizer. In the transition mode, the channelized equalizer $\mathbf{C}_e$ has already converged based on five different propagation channels. In both receivers, the step size for the propagation channel equalizer is set to be 0.1. The step size for the channelizer equalizer is set to be 0.005 in transition mode and 0.2 in startup mode to accelerate the initial convergence.

The learning curves when $E_b/N_0 = 12dB$ are given in Fig. 4 and Fig. 5 for the FSE and SSE, respectively. The convergence speed of the channelized receiver in transition mode is approximately the same as that of the full band receiver. This result is not surprising since when operating in transition mode, the convergence speed is set predominantly by the propagation channel equalizer, which has the same structure as that of the full band receiver. At steady-state, the channelized receiver performs slightly worse than the full band receiver, because cascaded adaptive filters generally suffer from additional excess MSE. The minimum MSE is lower in the FSE than in the SSE, since the SSE is suboptimal.

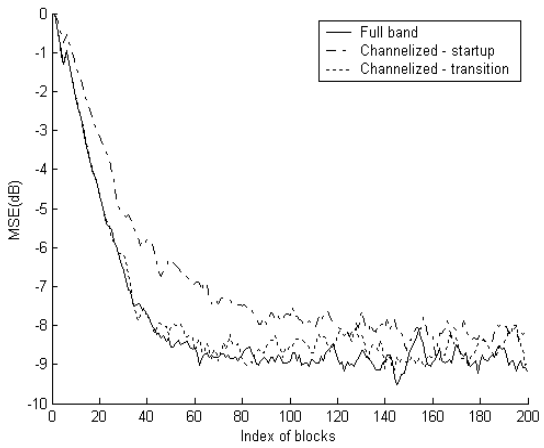

Fig. 4 MSE learning curves of FSE

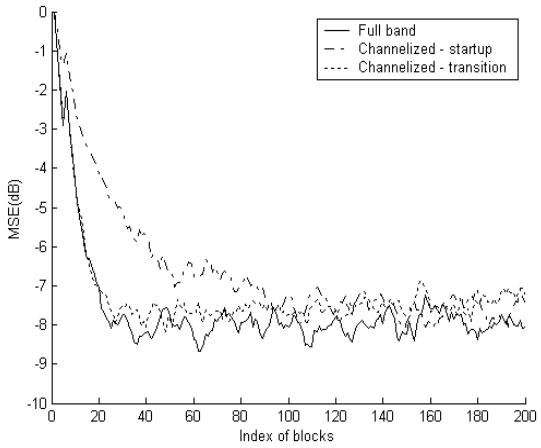

Fig. 5 MSE learning curves of SSE

The bit error rate (BER) of FSE and SSE are compared in Fig. 6. The channel is assumed to be constant during a packet consisting of 200 transmission blocks. In each packet, the first block is used for training. The channelized receiver is assumed to operate in the transition mode. The performance of the channelized receiver and the full band receiver is similar for both the FSE and SSE. Although the SSE converge faster as shown in the previous figures, the FSE receiver outperforms the SSE receiver significantly when only one training block is employed.

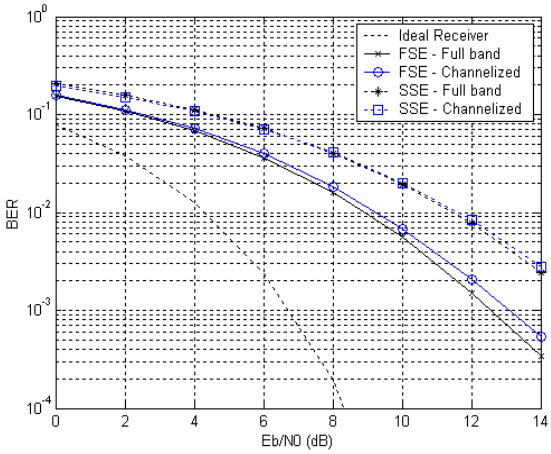

Fig. 6 BER of FSE and SSE with 1 training block

In Fig. 7, the BER performance of the FSE for both channelized and full band receivers are simulated for a packet consisting of 200 transmission blocks where the first 1 and 10 blocks are used for training. The channelized receiver operates in the transition mode. The channelized receiver performance is similar to that of the full band receiver especially when E_b/N_0 is low to moderate.

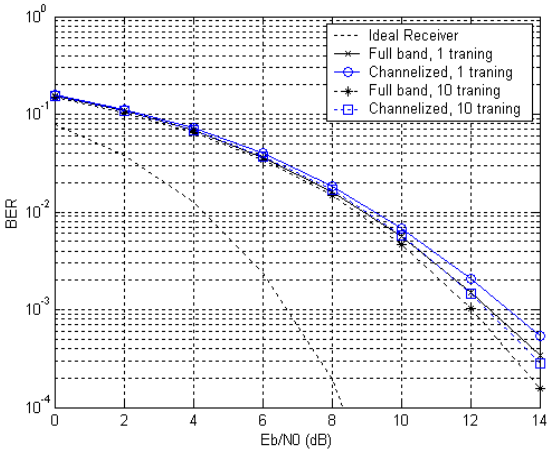

Fig. 7 FSE with 1 and 10 training blocks

6 CONCLUSIONS

Adaptive FSE and SSE algorithms for maximally decimated UWB channelized receivers with CP transmission are derived. Applying CP to the transmitted data enables the channelizer to be modeled as a BCM and the propagation channel to be modeled as a CM. By exploiting the modulation relations among the subbands, the BCM is diagonalized. As a result, equalization for the channelized receiver is achieved by cascading two one-tap equalizers, one of which corresponds to the channelizer and the other to the propagation channel. This decomposition allows the propagation channel and channelizer equalizers to be updated at different rates. After initial convergence of the channelizer equalizer, the performance of the channelized receiver is similar to that of an ideal full band receiver.

APPENDIX

The cost function is defined as the squared error

$$\begin{aligned} J &= \mathbf{e}_a^H \mathbf{e}_a \\ &= \mathbf{a}^H\mathbf{a} - \mathbf{a}^H\hat{\mathbf{a}} - \hat{\mathbf{a}}^H\mathbf{a} + \hat{\mathbf{a}}^H\hat{\mathbf{a}} \end{aligned} \tag{45}$$

To simply notations, define

$$\mathbf{p} = (\mathbf{F}_B^{-1})^H \mathbf{F}^H \left[\Lambda_{e0}^H \ \Lambda_{e1}^H\right]^H (\mathbf{F}_{1/2}^{-1})^H \mathbf{a},$$

$$\mathbf{q} = \mathbf{F}_D^{-1}\mathbf{F}_B\mathbf{x} \quad \text{and}$$

$$\mathbf{R}_\Lambda = (\mathbf{F}_B^{-1})^H \mathbf{F}^H \left[\Lambda_{e0}^H \ \Lambda_{e1}^H\right]^H \left[\Lambda_{e0}^H \ \Lambda_{e1}^H\right] \mathbf{F}\mathbf{F}_B^{-1}.$$

For FSE,

$$-\mathbf{a}^H\hat{\mathbf{a}} = -\frac{1}{2}\mathbf{p}^H\mathbf{C}_e^H\mathbf{q} \tag{46}$$

$$-\hat{\mathbf{a}}^H\mathbf{a} = -\frac{1}{2}\mathbf{q}^H\mathbf{C}_e\mathbf{p} \tag{47}$$

$$\hat{\mathbf{a}}^H\hat{\mathbf{a}} = \frac{1}{2MN}\mathbf{q}^H\mathbf{C}_e\mathbf{R}_\Lambda\mathbf{C}_e^H\mathbf{q} \tag{48}$$

Because $\nabla_\lambda \mathbf{a}^H\mathbf{a} = \nabla_c \mathbf{a}^H\mathbf{a} = 0$, the gradients with respect to $\mathbf{c}$ are

$$\nabla_c(-\mathbf{a}^H\hat{\mathbf{a}}) = -\mathbf{q} \bullet \mathbf{p}^* \tag{49}$$

$$\nabla_c(-\hat{\mathbf{a}}^H\mathbf{a}) = 0 \tag{50}$$

$$\nabla_c(\hat{\mathbf{a}}^H\hat{\mathbf{a}}) = \frac{1}{MN}\mathbf{q} \bullet \frac{\partial}{\partial(\mathbf{C}_e^H\mathbf{q})}(\mathbf{q}^H\mathbf{C}_e\mathbf{R}_\Lambda\mathbf{C}_e^H\mathbf{q}) = \frac{1}{MN}\mathbf{q} \bullet (\mathbf{R}_\Lambda^H\mathbf{C}_e^H\mathbf{q})^* \tag{51}$$

Summing (49), (50) and (51), the gradient of J with respect to $\mathbf{c}$ is

$$\nabla_c J = \mathbf{q} \bullet (\mathbf{p} - \mathbf{R}_\Lambda^H\mathbf{C}_e^H\mathbf{q})^* \tag{52}$$

To compute $\nabla_\lambda J$, define $\mathbf{y} = (\mathbf{F}_{1/2}^{-1})^H\mathbf{a}$ and $\mathbf{z} = \mathbf{F}\mathbf{F}_B^{-1}\mathbf{C}_e^H\mathbf{F}_D^{-1}\mathbf{F}_B\mathbf{x}$. $\mathbf{z}$ can be expressed as two $MN/2 \times 1$ vector $\mathbf{z} = \begin{bmatrix}\mathbf{z}_0^T & \mathbf{z}_1^T\end{bmatrix}^T$

Gradients with respect to λ are

$$\nabla_\lambda(-\mathbf{a}^H\hat{\mathbf{a}}) = 2\frac{\partial}{\partial\lambda^*}\left(-\frac{1}{2}\mathbf{y}^H\begin{bmatrix}\Lambda_{e0}^H & \Lambda_{e1}^H\end{bmatrix}\mathbf{z}\right) = -\mathbf{z} \bullet \begin{bmatrix}\mathbf{y}\\ \mathbf{y}\end{bmatrix}^* \tag{53}$$

$$\nabla_\lambda(-\hat{\mathbf{a}}^H\mathbf{a}) = 2\frac{\partial}{\partial\lambda^*}\left(-\frac{1}{2}\mathbf{z}^H\begin{bmatrix}\Lambda_{e0}^H & \Lambda_{e1}^H\end{bmatrix}^H\mathbf{y}\right) = 0 \tag{54}$$

$$\nabla_\lambda(\hat{\mathbf{a}}^H\hat{\mathbf{a}}) = \frac{1}{MN}\frac{\partial}{\partial\lambda^*}\left(\begin{bmatrix}\mathbf{z}_0^H & \mathbf{z}_1^H\end{bmatrix}\begin{bmatrix}\Lambda_{e0}\\ \Lambda_{e1}\end{bmatrix}\begin{bmatrix}\Lambda_{e0}^H & \Lambda_{e1}^H\end{bmatrix}\begin{bmatrix}\mathbf{z}_0\\ \mathbf{z}_1\end{bmatrix}\right) = z \bullet \begin{bmatrix}\frac{1}{MN}\begin{bmatrix}\Lambda_{e0}^H & \Lambda_{e1}^H\end{bmatrix}\mathbf{z}\\ \frac{1}{MN}\begin{bmatrix}\Lambda_{e0}^H & \Lambda_{e1}^H\end{bmatrix}\mathbf{z}\end{bmatrix}^* \tag{55}$$

Summing (53), (54) and (55), the gradient of J with respect to λ is

$$\nabla_\lambda J = -\mathbf{z} \bullet \begin{bmatrix}\mathbf{y} - \frac{1}{MN}\begin{bmatrix}\Lambda_{e0}^H & \Lambda_{e1}^H\end{bmatrix}\mathbf{z}\\ \mathbf{y} - \frac{1}{MN}\begin{bmatrix}\Lambda_{e0}^H & \Lambda_{e1}^H\end{bmatrix}\mathbf{z}\end{bmatrix}^* \tag{56}$$

For SSE, $-\mathbf{a}^H\hat{\mathbf{a}}$, $-\hat{\mathbf{a}}^H\mathbf{a}$ and $\hat{\mathbf{a}}^H\hat{\mathbf{a}}$ are of the same form as (46)-(48) except that $[\Lambda_{e0}^H \ \Lambda_{e1}^H]$ is replaced by $\Lambda_s^H[\rho_0^H \ \rho_1^H]$. $\nabla_{sc}J$, the gradient of J with respect to each equalization tap of $\mathbf{C}_e^H$, is readily obtained from (52) with the same replacement. We omit the equation here. Gradients of the three terms with respect to each equalization tap of Λ_s^H are

$$\nabla_{s\lambda}(-\mathbf{a}^H\hat{\mathbf{a}}) = -\begin{bmatrix}\rho_0^H & \rho_1^H\end{bmatrix}\mathbf{z} \bullet \mathbf{y}^* \tag{57}$$

$$\nabla_{s\lambda}(-\hat{\mathbf{a}}^H\mathbf{a}) = 0 \tag{58}$$

$$\nabla_{s\lambda}(\hat{\mathbf{a}}^H\hat{\mathbf{a}}) = \begin{bmatrix}\rho_0^H & \rho_1^H\end{bmatrix}\mathbf{z} \bullet \left[\frac{1}{MN}\Lambda_s^H\begin{bmatrix}\rho_0^H & \rho_1^H\end{bmatrix}\mathbf{z}\right]^* \tag{59}$$

The gradient of J with respect to the taps of Λ_s^H for SSE is

$$\nabla_{s\lambda}J = -\begin{bmatrix}\rho_0^H & \rho_1^H\end{bmatrix}\mathbf{z} \bullet \left[\mathbf{y} - \frac{1}{MN}\Lambda_s^H\begin{bmatrix}\rho_0^H & \rho_1^H\end{bmatrix}\mathbf{z}\right]^* \tag{60}$$

REFERENCES

[1] W. Namgoong, "A Channelized Digital Ultra-Wideband Receiver," IEEE Trans. Wireless Comm., vol. 2, pp. 502-510, May 2003

[2] S. R. Velazquez, T. Q. Nguyen and S. R. Broadstone, "Design of Hybrid Filter Banks for Analog/Digital Conversion," IEEE Trans. on Signal Processing, vol. 46 NO. 4, pp.956 - 967, Apr. 1998

[3] P. Lowenborg, H. Johansson and L. Wanhammar, "Two-Channel Digital and Hybrid Analog/Digital Multirate Filter Banks With Very Low-Complexity Analysis or Synthesis Filters," IEEE Trans. on Circuits and Systems II: Analog and Digital Signal Processing, vol. 50, NO. 7, pp.355 - 367, Jul. 2003

[4] A. Gilloire and M. Vetterli, "Adaptive Filtering in Subbands with Critical Sampling: Analysis, Experiments, and Application to Acoustic Echo Cancellation," IEEE Trans. on Signal Proc. vol. 40, NO. 8, pp.1862 - 1875, Aug. 1992

[5] L. Feng and W. Namgoong, "A frequency channelized adaptive wideband receiver for high-speed links," Signal Processing Systems, 2003. SIPS 2003. IEEE Workshop on, pp. 24 -28, Aug. 2003

[6] J.A. C. Bingham, "Multicarrier Modulation for Data Transmission: An Idea whose Time has Come," IEEE Comm. Magazine, vol. 28, NO. 5, pp. 5-14, 1990

[7] J. Louveaux, L. Vandendorpe and T. Sartenaer, "Cyclic Prefixed Single Carrier and Multicarrier Transmisson: Bit Rate Comparison," IEEE Comm. Letters, vol. 7, NO. 4, pp. 180 - 182, Apr. 2003

[8] D. Falconer, et al, "Frequency Domain Equalization for Single-Carrier Broadband Wireless Systems," IEEE Comm. Mag., pp.58 - 66, Apr. 2002

[9] R. Harjani, J. Harvey and R. Sainati, "Analog/RF Physical Layer Issues for UWB Systems," VLSI Design, 2004. Proceedings. 17th International Conference on, pp.941 - 948, 2004

[10] R. Vescovo, "Inversion of Block-Circulant Matrices and Circular Array Approach," IEEE Trans. on Antennas and Propagation, vol. 45, NO. 10, pp.1565 - 1567, Oct. 1997

[11] T. De Mazancourt and D. Gerlic, "The Inverse of a Block-circulant Matrix," IEEE Trans. Antennas Propagat., vol. AP-31, pp.808-810, Sept. 1983

[12] P.P. Vaidyanathan and B. Vrcelj, "Theory of Fractionally Spaced Cyclic-Prefix Equalizers," ICASSP'02, vol.2, pp. 1277-1280, 2002

[13] H. Meyr, M. Moeneclaey and S. A. Fehtel, "Digital Communication Receivers: Synchronization, Channel Estimation, and Signal Processing," John Wiley & Sons, Inc. 1998

[14] J. G. Proakis, “Digital Communications, Third Edition”, McGraw-Hill, 1998

Lei Feng (S’03) received the B.S. and M.S. degree in electrical engineering from Peking University, Beijing, in 1997 nad 2000, respectively. He is currently working toward the Ph.D degree in electrical engineering at University of Southern California, Los Angeles, CA. His doctoral research focuses on the design of wideband communication transceivers for wireless and wireline applications.

Won Namgoong received the BS degree in Electrical Engineering and Computer Science from the University of California at Berkeley in 1993, and the MS and Ph.D. degrees in Electrical Engineering from Stanford University in 1995 and 1999, respectively. In 1999, he joined the faculty of the Electrical Engineering Department at the University of Southern California, where he is an Assistant Professor. His current research areas include wireless/wireline communication systems, signal processing systems, RF circuits, and low-power/high-speed circuits. In 2002, he received the National Science Foundation (NSF) CAREER Award. He currently serves as the Associate Editor of IEEE Transactions on Circuits and Systems I - Regular Papers.